The longtime behavior of reversible binary reactions: Theory, Brownian simulations and experiment

Noam Agmon and Arieh L. Edelstein

Citation: The Journal of Chemical Physics **100**, 4181 (1994); doi: 10.1063/1.466302
View online: http://dx.doi.org/10.1063/1.466302
View Table of Contents: http://scitation.aip.org/content/aip/journal/jcp/100/6?ver=pdfcov
Published by the AIP Publishing

The long-time behavior of reversible binary reactions: Theory, Brownian simulations and experiment

Noam Agmon and Arieh L. Edelstein
Department of Physical Chemistry and the Fritz Haber Research Center, The Hebrew University, Jerusalem 91904, Israel

(Received 21 October 1993; accepted 2 December 1993)

Many-body effects on reversible pseudo-unimolecular reactions are investigated using a combination of theory, simulation, and experiment. Theoretically, we rederive the superposition approximation starting from the fundamental N-particle equations. All the relations obtained are actually rigorous, except for a requirement that the concentration profile outside a vacant trap obeys a diffusion equation. Our derivation also yields a new numerical procedure for evaluating the superposition solution. Brownian dynamics simulations of one-dimensional competitive binding are presented over an unprecedented time regime. Comparison with the superposition approximation shows that this mean-field theory is exact at infinite dilution, but breaks down at high particle concentration. The main discrepancy is not at asymptotically long times as previously suspected, but rather at intermediate times, where a new power law-phase emerges. This is reflected in a maximum in the logarithmic derivative of the survival probability, which is more pronounced in our simulation as compared with the approximate theory. Finally, we show that the transient fluorescence data from an excited dye molecule which transfers a proton reversibly to water, develops a similar maximum in its logarithmic derivative at low pH values.

I. INTRODUCTION

The treatment of reversible bimolecular reactions in solution poses an intricate many-body problem. Theoretical work has suggested several approximate approaches.[1–10] Lee and Karplus[1] have generalized the hierarchal approach of Waite[11] and others[12,13] to reversible reactions. This approach begins with equations of motion for pair, triplet, and higher probability density functions. Szabo and Zwanzig[5] developed a discrete occupation number formalism for the pseudo-unimolecular case of a single, static reversible trap ("competitive binding"). In both approaches the hierarchy is truncated using a superposition approximation (SA).[11,12]

The SA has been shown[5,6] to be a very reasonable approximation, becoming exact in the limits of infinite dilution and infinite times. While it is evident that as $t\to\infty$ the SA tends to the correct equilibrium limit, it is not altogether clear whether it does so with the correct time dependence: The SA predicts a power-law, $t^{-d/2}$, approach of the binding probability to its equilibrium value with a universal power, $d/2$, which depends only on the spatial dimensionality, d, but not on the particle concentration, c. In this picture, the asymptotic behavior of a geminate pair[14] extends to the many-body case.

It is interesting that such a prediction could be checked experimentally:[15] The transient fluorescence from an excited dye molecule which transfers a proton reversibly to its aqueous environment has been monitored as a function of the solution pH. With increasing proton concentration, the asymptotic slope seemed to increase *above* the theoretical value of 3/2. A question arises whether this apparent disagreement is due to the breakdown of the SA, limitations of the experimental accuracy or both.

We begin (Sec. II) by rederiving the SA from the fundamental diffusion equations governing the time evolution of the N-particle probability distribution function.[10] The hierarchal approaches[1,9] are a special case obtained by partial integration of these basic equations. The occupation number formalism[5] is also a special case, valid in the discrete case of equivalent particles, namely, identical particles all starting from identical initial conditions. The general equations may, however, be treated along alternate routes such as the generalization of the kinetic density expansion[16] to the reversible case.[10] By iteratively integrating out N, $N-1$, and $N-2$ out of the N-particle coordinates, we show how the three decoupling assumptions involved in the SA[5,9] may be replaced by the single requirement that the conditional particle density outside a free trap obeys a diffusion equation. This suggests possible routes for obtaining higher correction terms.

In order to clarify the apparent discrepancy between experiment and the SA, we have developed a Brownian dynamics algorithm for reversible reactions which allows accurate simulation of the many-particle dynamics over many orders of magnitude in time.[17] The algorithm has been implemented in one dimension, for which a comprehensive set of simulations is presented below (Sec. III). These are compared with numerical solutions of the SA, calculated using a novel numerical procedure.

A central finding in this work is that at high concentrations there are actually *two* power-law phases with an intermediate-time power which is indeed larger than $d/2$. In other words, the logarithmic derivative of the survival probability ("beta function") goes through a maximum which, at high concentrations, is much more pronounced in the simulations than in the SA. At still longer times both seem to tend to the universal $d/2$ limit. We evaluate the

 0021-9606/94/100(6)/4181/7/$6.00

beta function of the experimental data[15] finding that it reveals similar trends (Sec. IV).

II. THEORY

We consider N identical diffusing particles with a reversible trap at the origin. For simplicity, we assume one-dimensional motion on a line segment $[0,L]$, although the theory can be easily generalized to three dimensions. Also, we assume the particles are noninteracting although the theory can be generalized to include trap-particle interactions. These restrictions will allow us to focus primarily on the many-body aspects of the problem. The trap can bind at most one particle ("competitive binding"). When no particle is bound, trapping may occur at $x=0$ (the "contact distance") with the recombination rate coefficient κ_r. When a particle is bound, the boundary at $x=0$ becomes reflective. A bound particle may in turn, dissociate to contact with a rate coefficient κ_d.

Our starting point is the N-particle diffusion equation for the joint probability density $p_N(x_1,...,x_N;t)$, where $0\leqslant x_i\leqslant L$ is the distance of the ith particle from the origin. In our notation,[10] x_i may also assume one discrete value, $*$, representing a bound particle. Thus $p_N(*,x_2,...,x_N;t)$ is the probability density for diffusing particles 2,... ,N given that particle 1 is bound at time t. It has units of $1/L^{N-1}$ whereas $p_N(x_1,x_2,...,x_N;t)$ has units of $1/L^N$. For a single-particle trap, the probability of events such as $(*,*,x_3,...,x_N)$ vanishes. The probability density normalizes to unity when integrated over both free and bound states.

When no particle is bound, the basic equation of motion is

$$\partial p_N(x_1,...,x_N;t)/\partial t=\sum_{i=1}^{N}\mathcal{L}_i p_N(x_1,...,x_N;t),\qquad 0\leqslant x_j\leqslant L\,. \tag{1a}$$

For noninteracting point particles in one-dimension, $\mathcal{L}_i\equiv D\,\partial^2/\partial x_i^2$ is the diffusion operator for particle i and D its diffusion constant. The forthcoming equations are subject to the following notational conventions: (i) $i=1,...,N$; (ii) $j\neq i$, and (iii) $0\leqslant x_j\leqslant L$ (i.e., $x_j\neq *$).

Equation (1a) resembles the starting point in the treatment of irreversible reactions by Monchick *et al.*[12] It needs to be generalized to the reversible case.[10] First, consider the boundary conditions imposed on it. The outer boundary conditions are reflective

$$\partial p_N(x_1,...,x_N;t)/\partial x_i|_{x_i=L}=0\,, \tag{1b}$$

representing the finite size of the system. Eventually we will take both N and L to infinity, keeping the particle concentration, $c\equiv N/L$, constant (the "thermodynamic limit"). The boundary condition at the trap depicts back reaction[18] in each and every coordinate

$$D\,\partial p_N(...,x_i,...;t)/\partial x_i|_{x_i=0}=\kappa_r p_N(...,x_i=0,...;t)-\kappa_d p_N(...,x_i=*,...;t). \tag{1c}$$

The "intrinsic" recombination and dissociation rate coefficients are denoted by κ_r and κ_d, respectively. They represent transitions between the bound ($x_i=*$) and contact ($x_i=0$) states. Equation (1c) reduces to the irreversible, "radiation" boundary condition when $\kappa_d=0$.

The density function given that particle i is bound obeys a diffusion equation in the remaining $N-1$ coordinates. In addition, it may increase or decrease due to association or dissociation of particle i. Therefore[10]

$$\partial p_N(...,x_i=*,...;t)/\partial t=\sum_{j\neq i=1}^{N}\mathcal{L}_j p_N(...,x_i=*,...;t)+\kappa_r p_N(...,x_i=0,...;t)-\kappa_d p_N(...,x_i=*,...;t). \tag{1d}$$

The last equation is again subject to boundary conditions, which are now reflective at *both* ends

$$\partial p_N(...,x_i=*,...;t)/\partial x_j|_{x_j=0,L}=0. \tag{1e}$$

Hence binding of a second particle is disallowed.

Two kinds of initial conditions are of interest:

(a) All N particles are initially equivalent and uncorrelated by virtue of being unbound and uniformly distributed,

$$p_N(x_1,...,x_N;0|\text{uni})=1/L^N\,. \tag{2}$$

This is the case more amenable to theoretical treatments.

(b) One particle is initially bound while the remaining $N-1$ particles are randomly distributed. This is the initial condition in the experimental setup.[15] The solutions for the two initial conditions are related by the generalized mass action law.[2,5,10] Whenever specification of the initial condition is important, we use the notations $(...;t|\text{uni})$ and $(...;t|*)$ for the initially uniform and bound cases, respectively. The equations as presented here are sufficiently general to treat nonequivalent particles, each starting from a different initial condition. When the initial condition is not specified, the result is understood to hold for an arbitrary initial condition.

A fundamental quantity of interest is the survival probability, namely, the probability that none of the N particles is bound at time t. It is defined by the N-fold integral

$$S_N(t)\equiv\int_0^L\cdots\int_0^L p_N(x_1,...,x_N;t)\prod_{i=1}^{N}dx_i. \tag{3}$$

It is often the survival probability (and rarely the density distribution itself) which is an experimental observable. The binding probability, namely, the probability that one out of the N particles is bound, is similarly defined by

$$q_N(t)\equiv\sum_{i=1}^{N}\int_0^L\cdots\int_0^L p_N(...,x_i=*,...;t)\prod_{j\neq i}dx_j=N\int_0^L\cdots\int_0^L p_N(*,x_2,...,x_N;t|\text{uni})\prod_{j=2}^{N}dx_j. \tag{4}$$

The first expression is general, while the second holds for equivalent particles (i.e., identical particles having the same initial condition). This follows because for equivalent

particles $p_N(...,x_i,...,x_j,...;t)=p_N(...,x_j,...,x_i,...;t)$. Since the trap may be either free or singly occupied, we expect that

$$S_N(t)=1-q_N(t)\ . \tag{5}$$

We will see below that this normalization condition is commensurate with the many-body equations (1a)–(1e). It may also be shown[10] that these equations tend to a true equilibrium state as $t\to\infty$, for which[2]

$$S_{eq}\equiv S_N(\infty)=(1+cK_{eq})^{-1},\quad K_{eq}\equiv\kappa_r/\kappa_d, \tag{6}$$

irrespective of the initial condition.

It is useful to introduce an integral over $N-1$ of the N free particle coordinates

$$\bar{P}_N(x;t)\equiv[c\,S_N(t)]^{-1}\sum_{i=1}^{N}\int_0^L\cdots\int_0^L p_N(...,x_i=x,...;t)\prod_{j\neq i}dx_j$$
$$=[L/S_N(t|\mathrm{uni})]\int_0^L\cdots\int_0^L p_N(x,x_2,...,x_N;t|\mathrm{uni})\prod_{j=2}^{N}dx_j. \tag{7}$$

The second line again refers to the special case of equivalent particles. From a physical point of view, $c\,\bar{P}_N(x;t)$ is the concentration profile of particles outside a free trap. It is a *conditional* particle density, conditioned on the trap being vacant.[1,9] The $N-1$ dimensional integral in Eq. (7) is the probability density for particle i to be unbound and at a distance x from the trap. It may thus be identified with $P_{A_i,B_j}(x,y,t)$ of Lee and Karplus[1] in the special case of a single, stationary B particle ("the trap") at $y=0$.

From Eq. (3), $\int_0^L\bar{P}_N(x;t)\,dx=L$. Hence $\bar{P}_N(x;t)/L$ is a *conditional* probability density which normalizes to unity at all times. For an initial uniform distribution Eq. (2) implies that $\bar{P}_N(x;0|\mathrm{uni})=1$. As $t\to\infty$, the density becomes constant [see Eq. (5.1) in Ref. 10], $p_N(x_1,...,x_N;\infty)=[(1+cK_{eq})\,L^N]^{-1}$. Therefore $\bar{P}_{eq}(x)\equiv\bar{P}_N(x;\infty)=1$. Starting from a uniform distribution, $\bar{P}_N(x;t|\mathrm{uni})$ initially is unity everywhere. Due to the binding process, it subsequently decreases near the trap and increases at larger distances, keeping its area constant. Finally, it becomes unity once more.

Our first step is to generate an equation of motion for $S_N(t)$ by differentiating its definition (3) with respect to time

$$\frac{dS_N(t)}{dt}=\sum_{i=1}^{N}\int_0^L\cdots\int_0^L[-\kappa_r p_N(...,x_i=0,...;t)$$
$$+\kappa_d p_N(...,x_i=*,...;t)]\prod_{j\neq i}dx_j. \tag{8}$$

To obtain this result, we have used the many-body diffusion equation (1a) and the boundary condition (1c). Next, by inserting Eqs. (1d) and (1e) into Eq. (8) and integrating, one obtains $dS_N(t)/dt=-dq_N(t)/dt$, in agreement with the normalization condition (5). Substituting Eqs. (4), (5), and (7) into (8) gives

$$dS_N(t)/dt=-c\kappa_r S_N(t)\bar{P}_N(0;t)+\kappa_d[1-S_N(t)]\ . \tag{9}$$

This rate-equation like expression has been obtained by several groups.[1,2,5,9] Our derivation shows that it is rigorously valid for *any* initial condition and any number of particles, provided that $\bar{P}_N(x;t)$ is related to the N-particle density via Eq. (7).

Equation (9) requires the exact form for $\bar{P}_N(x;t)$. We therefore seek an equation of motion for it. By differentiating Eq. (7) with respect to time and using the N-body diffusion equation (1a), one gets

$$\frac{\partial\bar{P}_N(x;t)}{\partial t}=\mathscr{L}\,\bar{P}_N(x;t)-\bar{P}_N(x;t)\frac{d\ln S_N(t)}{dt}$$
$$+\sum_{i=1}^{N}\int_0^L\cdots\int_0^L\sum_{j\neq i}\frac{\mathscr{L}_j p_N(...,x_i=x,...;t)}{c\,S_N(t)}\prod_{j\neq i}dx_j\ . \tag{10}$$

This result is again exact for any initial condition of unbound particles. After some manipulations it can be seen to be equivalent to Eq. (2.61) of Lee and Karplus.[1] Here it is derived from the fundamental equations (1a)–(1e) rather than been a postulated starting point.

The boundary condition imposed on $\bar{P}_N(x;t)$ at $x=0$ can also be found by differentiating Eq. (7). Inserting the back-reaction boundary condition (1c) and using Eqs. (8) and (9) gives

$$D\frac{\partial\bar{P}_N(x;t)}{\partial x}\bigg|_{x=0}=-c^{-1}\frac{d\ln S_N(t)}{dt}$$
$$=\kappa_r\bar{P}_N(0;t)-\kappa_d\frac{[1-S_N(t)]}{cS_N(t)}\ . \tag{11a}$$

While this boundary condition is equivalent to Eq. (4.39) in Szabo and Zwanzig,[5] it is again seen to be exact, not an approximation. Introducing the notation $\bar{P}_N(*;t)$, Eq. (11a) becomes *almost* equivalent to single-particle dynamics [Eqs. (1c)–(1d) for $N=1$]. Indeed, setting $x=*$ in

definition (7) gives $\bar{P}_N(*;t)=[1-S_N(t)]/cS_N(t)$ or $S_N(t)=[1+c\bar{P}_N(*;t)]^{-1}$. Inserting into Eq. (11a) yields

$$D\frac{\partial \bar{P}_N(x;t)}{\partial x}\bigg|_{x=0} = S_N(t)\frac{d\bar{P}_N(*;t)}{dt}$$

$$= \kappa_r \bar{P}_N(0;t) - \kappa_d \bar{P}_N(*;t)\,. \qquad (11b)$$

While the flux is given by a back-reaction term, it is not equal to the time derivative $d\bar{P}_N(*;t)/dt$ due to the extra $S_N(t)$ factor. With the identification $\phi(t)\equiv\bar{P}_N(*;t)$, the second equality in Eq. (11b) is the same as Eq. (3.13) in Szabo and Zwanzig,[5] after correcting a typographical error there.

The SA can now be characterized as a replacement of $\bar{P}_N(x;t)$ by an approximate form, $\bar{P}_{SA}(x;t)$, obtained from an approximate equation of motion,

$$\partial\bar{P}_{SA}(x;t)/\partial t = \mathscr{L}\,\bar{P}_{SA}(x;t)\,, \qquad (12)$$

which constrains the particle density outside a free trap to obey a diffusion equation. This is a mean-field type of approximation expected to be useful in the thermodynamic limit. In going from Eq. (10) to Eq. (12) one drops the N-dependent term, therefore the subscript N may be replaced by the subscript SA.

Equation (12) holds if the last two terms in Eq. (10) vanish identically (the SA condition). Insertion of Eqs. (1c) and (8) into Eq. (10) yields two terms proportional to κ_d and κ_r, respectively. Since the two rate parameters may be varied independently, the SA condition requires that each of their coefficients vanishes. For equivalent particles this gives

$$\int_0^L\cdots\int_0^L p_N(x,0,\ldots,x_N;t|\text{uni})\prod_{j=3}^{N}dx_j$$

$$\approx S_{SA}(t)\,\bar{P}_{SA}(x;t)\,\bar{P}_{SA}(0;t)\,/L^2\,, \qquad (13a)$$

$$c\int_0^L\cdots\int_0^L p_N(x,*,\ldots,x_N;t|\text{uni})\prod_{j=3}^{N}dx_j$$

$$\approx [1-S_{SA}(t)]\bar{P}_{SA}(x;t)\,/L^2\,. \qquad (13b)$$

In this derivation one replaces $N-1$ by N assuming approach to the thermodynamic limit. Conditions (13) depict the two particle density functions on the l.h.s. as superpositions of one particle functions on the r.h.s.[11,12] For example, approximation (13a) states that the probability of having a free trap with particle 1 at x and particle 2 at contact is the probability for a free trap *times* the conditional probabilities of a particle at x and a particle at contact. This can be expected to become exact in the limit of infinite dilution ($c\to 0$) when the particles become independent of each other. It is interesting to compare Eq. (13) with Eq. (4.35) of Szabo and Zwanzig[5] or Eq. (B5) of Naumann:[9] Of the three assumptions listed there, one is merely the definition of $\bar{P}_N(x;t)$ while another may be weakened since Eq. (13a) involves one particle at x and another at $x=0$.

In the thermodynamic limit, the SA requires[6] the solution of the coupled ordinary and partial differential equations (9) and (12), the latter subject to the boundary condition (11a). For a finite system, Eq. (11b) suggests modifying the boundary condition (11a) so that the partial differential equation (12) depicts effective single particle (ESP) dynamics. If in the limit of an infinite system the ESP solution will approach the SA, we will obtain an alternate route to that of Szabo[6] for evaluating the SA.

In the ESP dynamics, $\bar{P}_{SA}(*;t)$ and $\bar{P}_{SA}(x;t)$ are interpreted as the probability and probability density for the bound and unbound states, respectively. Therefore, we demand that they normalize *together* to some constant,

$$\bar{P}_{SA}(*;t)\equiv\int_0^L[\bar{P}_{SA}(x;0)-\bar{P}_{SA}(x;t)]\,dx\,. \qquad (14)$$

For an initial uniform distribution, $\bar{P}_{SA}(x;0)=1$ while $\bar{P}_{SA}(*;0)=0$. Clearly, Eq. (14) cannot hold for the exact $\bar{P}_N(x;t)/L$, which normalizes to unity at all times by definition (7). However, letting $L\to\infty$, $\bar{P}_{SA}(*;t)$ remains finite so that $\bar{P}_{SA}(*;t)/L\to 0$ and the normalization of $\bar{P}_{SA}(x;t)/L$ does become arbitrarily close to unity.

Since the approximate solution, $\bar{P}_{SA}(x;t)$, violates definition (7), we seek another relation between $\bar{P}_{SA}(*;t)$ and $S_{SA}(t)$. Differentiating Eq. (14) with respect to time and using first Eq. (12) and subsequently (11a), one finds that

$$\frac{d\bar{P}_{SA}(*;t)}{dt} = -\frac{\partial\int_0^L\bar{P}_{SA}(x;t)\,dx}{\partial t}$$

$$= D\frac{\partial\bar{P}_{SA}(x;t)}{\partial x}\bigg|_{x=0} = -c^{-1}\frac{d\ln S_{SA}(t)}{dt}\,. \qquad (15)$$

Hence unlike the exact solution, $\bar{P}_N(*;t)$ in Eq. (11b), the time derivative of $\bar{P}_{SA}(*;t)$ does equal to the flux term at contact. This term may be interpreted as a time-dependent rate-coefficient [Eq. (4.10) in Ref. 10]. Given the initial condition, Eq. (15) is integrated to yield

$$S_{SA}(t)=\exp[-c\,\bar{P}_{SA}(*;t)]\,. \qquad (16)$$

Subsequently, Eq. (11a) is replaced by the nonlinear ESP boundary condition

$$D\partial\bar{P}_{SA}(x;t)/\partial x|_{x=0}$$

$$=\kappa_r\bar{P}_{SA}(0;t)-\kappa_d[\exp(c\bar{P}_{SA}(*;t))-1]/c. \qquad (17)$$

Unlike the "bimolecular boundary condition"[7] and the "chemical approximation,"[5] which involve nonlinearities in the recombination term, here the nonlinearity occurs in the *dissociation* term. Our experience in such cases indicated that nonlinearities which appear only in the boundary condition may still allow large time steps to be taken. Hence the usefulness of the ESP approach. For small c, Eq. (17) reduces to the linear back-reaction boundary condition (11b) and the SA becomes exact. For large t, equating (17) to zero gives the correct equilibrium limit, Eq. (6), only if $\bar{P}_{SA}(0;t)\to 1$. As discussed following Eq. (14), this holds only in the thermodynamic limit. The ESP dynamics will not reproduce the correct equilibrium limit in a small finite system, but will do so with increasing system size.

To summarize, the ESP representation of the SA involves solving the diffusion equation (12) subject to the nonlinear boundary condition (17) and the normalization condition (14). The survival probability is eventually calculated from Eq. (16). This scheme is discretized on a line segment of the same length, L, as used in our Brownian simulations (Sec. III). The ensuing nearest-neighbor master equation has just one transition probability ($*\to 0$) which is time dependent. It is solved using Chebyshev propagation as discussed elsewhere.[19,7]

III. BROWNIAN DYNAMICS

The investigation of the long-time characteristics of reversible binding calls for long simulations of many particle diffusive dynamics. This is impractical using conventional random walk methods[5,7] which employ a small and fixed time step, Δt. We have recently developed a many-body Brownian dynamics algorithm to address this problem, which is described in detail elsewhere.[17]

Briefly, we assume that the single particle probability density, $p_1(x;\Delta t|x_0)$, for moving from point x_0 to x during the time interval Δt is known analytically, which is true for noninteracting particles in one dimension.[14,18] To simulate the N-particle dynamics, one particle is chosen at random and moved to a new location while keeping the remaining $N-1$ particles fixed. The endpoint of its trajectory is found by comparing a uniformly distributed random number, $0<\xi<1$, with the appropriate integral of the analytical single-particle solution. If the binding site is vacant and $\xi<p_1(*;\Delta t|x_0)$ the particle becomes bound and $x(t+\Delta t)=*$. If $\xi>p_1(*;\Delta t|x_0)$ it is moved to a new (unbound) location, x_ξ, which is found from

$$\xi-p_1(*;\Delta t|x_0)=\int_0^{x_\xi} p_1(x;\Delta t|x_0)\,dx\,. \tag{18}$$

This is a generalization of the procedure for selecting a random number out of a given distribution to the case that the distribution involves a continuous and a discrete part.

The single-particle move is repeated N times per Δt and mN times to reach time $t=m\Delta t$. This generates one N-particle stochastic trajectory, $(x_1(t),\ldots,x_N(t))$. The order of one million stochastic trajectories are averaged to give the binding probability with the desired (three-digit) accuracy. Different time windows are accessed using different $\Delta\ t$ values. After just a few ($m\approx 5$) time steps the calculation converges to that using a smaller $\Delta\ t$ value. The initial portion is discarded and the different pieces (typically 3–5) are connected together to produce the transient behavior over many orders of magnitude in time. The number of particles, N, and the interval length, L, are then doubled until the binding probability is invariant over the whole time regime of the simulation, $[0,t_{\max}]$. When this holds, the "thermodynamic limit" is said to be obtained for $t<t_{\max}$. The interval length, L, is thereafter kept constant and N is varied to check for concentration effects. It is clear that extensive numerical work is required to generate accurate data even with this efficient Brownian algorithm. The results shown below represent several months of continuous 486/50 MHz PC computations which, in the conventional random walk method, would have taken over 100 times longer to complete.

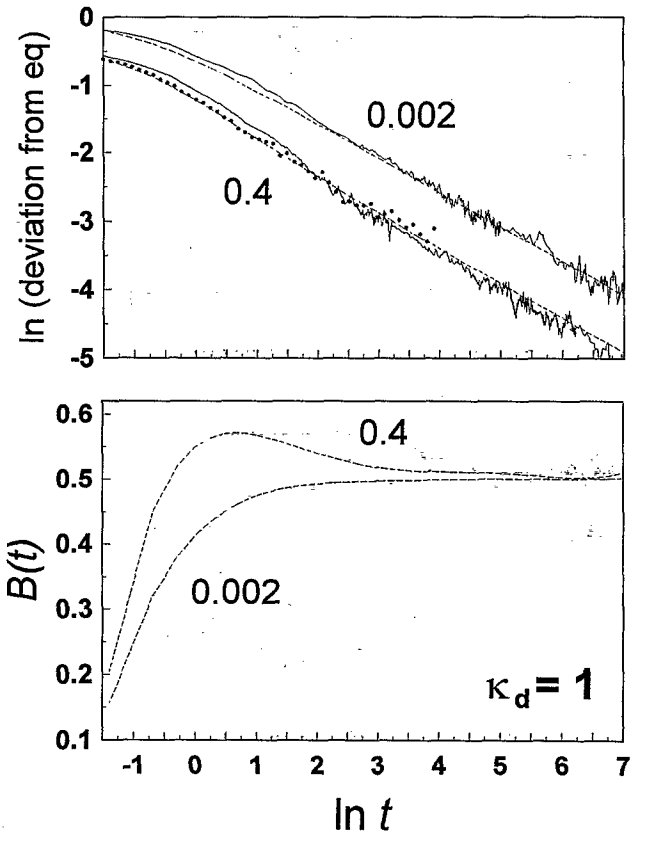

FIG. 1. The deviation from equilibrium, $S_{eq}-S_N(t|*)$, of the survival probability in one-dimensional Brownian simulations (full curves) compared with a numerical solution of the superposition approximation (dashed curves). In the simulation $D=1$, $\kappa_r=1$, and $L=2500$. The number of particles, N, is varied to obtain the concentrations quoted (in this case $N=5$ and 1000). Results for four different Δt values were stitched together to produce the dependence over nearly four decades of time (note the natural logarithmic scale). In addition, the short time behavior has been calculated using a discrete-time random walk program (Ref. 7). Results (circles) were obtained for periodic boundary conditions on a circle of length $2L$ with the dissociation parameter $\kappa_d/2$.

Figures 1 and 2 are the outcome of our Brownian simulations for two different values of the dissociation rate coefficient, κ_d. D and κ_r are set to unity, which is equivalent to choosing time and distance units. Simulated survival probabilities for a uniform initial distribution, $S_N(t|\text{uni})$, were converted to deviation from equilibrium for the experimentally relevant initially bound state using the generalized mass action law[2,5,10]

$$S_{eq}-S_N(t|*)=[S_N(t|\text{uni})-S_{eq}]/(c\,K_{eq})\,. \tag{19}$$

Here S_{eq} is the equilibrium limit of the survival probability, Eq. (6), as can be verified by setting $S_N(0|\text{uni})=1$ and $S_N(0|*)=0$. There is no error involved in applying Eq. (19), which is exact.

The (present version of the) Brownian dynamics program could be less accurate at short times, because

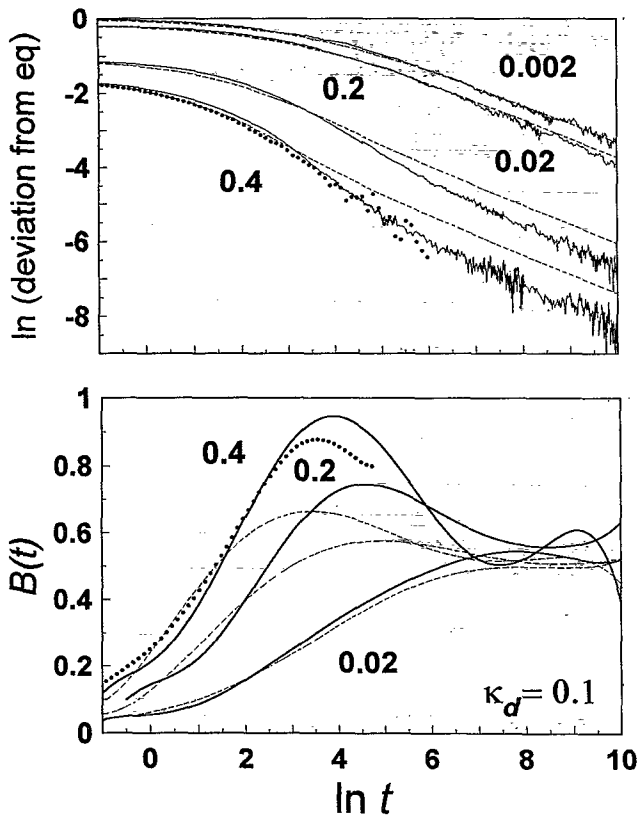

FIG. 2. Same as Fig. 1 for a larger value of cK_{eq}, showing enhanced maxima in $B(t)$ and observable deviations from the superposition approximation. In order to obtain $B(t)$ from the noisy simulation data, they were first fitted to eighth order polynomials which were then differentiated analytically (bold curves, bottom panel).

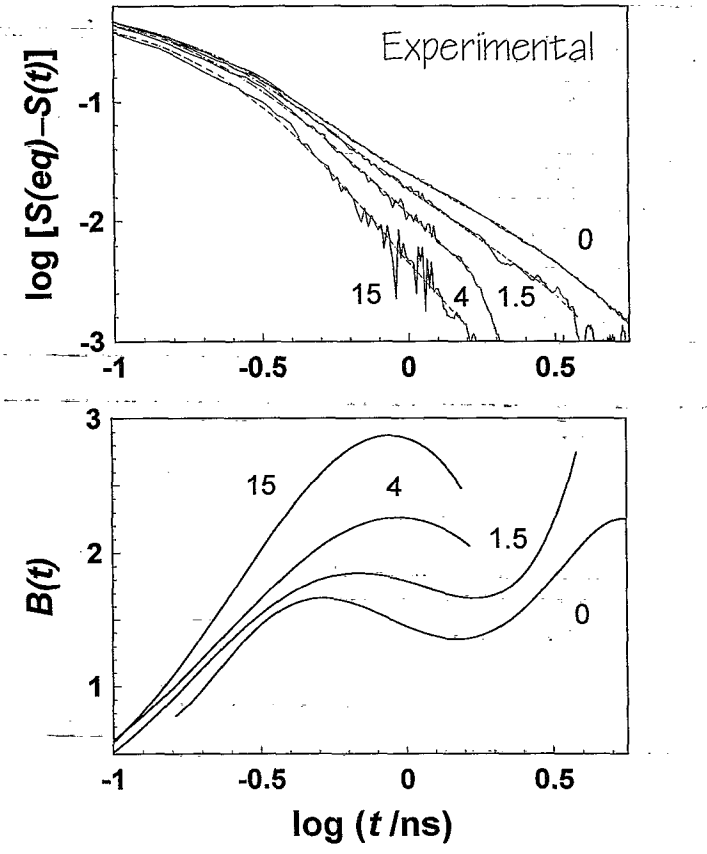

FIG. 3. The approach to equilibrium in reversible proton transfer to solvent from excited hydroxypyrene-trisulfonate. Time correlated single-photon counting data (bold curves, Ref. 15) have been corrected for the 6 ns radiative lifetime. Curves are labeled by the solution $[H^+]$ value in mM, the highest proton concentration corresponding to pH = 1.8. See text for additional detail.

$p_1(x;\Delta t|x_0)$ tends to a delta function with decreasing Δt rendering the integration in Eq. (18) inaccurate. As a check, the early time behavior for $c=0.4$ has been calculated using a more conventional lattice random-walk program (circles). This program[7] uses logarithmic time steps and may therefore be less accurate at long times. The best representation is achieved by using random walks for short times and the Brownian dynamics for long times.

The dashed curves in Figs. 1 and 2 show the corresponding behavior of the SA, calculated from the numerical solution of Eq. (12) subject to the boundary condition (17) and to Eqs. (14), (16), and (19). The SA is seen to be exact at infinite dilution but it breaks down at high concentrations. The relevant smallness parameter is[2] $cK_{eq} \equiv c\kappa_r/\kappa_d$. In Fig. 1 the largest value of cK_{eq} is 0.4 and the SA provides an excellent approximation over the whole time regime.[5] In Fig. 2, cK_{eq} goes up to 4. For $cK_{eq}=2$ there are already noticeable deviations from the SA. (Note, however, that the full SA calculations produce better agreement with the Brownian simulations as compared with the linearized SA[6] shown in our earlier work[17]). One concludes that $cK_{eq} \approx 1$ is an upper limit for SA validity.

In order to investigate the asymptotic slope more carefully we show, in the bottom panels of Figs. 1 and 2, the logarithmic derivatives

$$B(t) \equiv d \ln S(t|*)/d \ln t, \tag{20}$$

of the upper-panels' data. At asymptotically long times the SA tends to 1/2.[6] To within the statistical noise (ca. 20%), the exact simulations tend to the same universal power. If there is a variation with c, it is too small to be of practical significance in the parameter range investigated. The interesting new observation is the appearance of a maximum in $B(t)$ at intermediate times. The SA predicts not only the asymptotic slope correctly, but also the emergence of such a maximum at high concentrations. Quantitatively, this maximum is much more pronounced in the exact Brownian simulations once $cK_{eq} > 1$ (Fig. 2). Observed over a limited time regime, it may lead to the impression of an increasing asymptotic slope with increasing c.

IV. EXPERIMENT

Following the observations from our Brownian simulations we replot in Fig. 3 the experimental data of Ref. 15. These data involve reversible proton transfer from an excited dye molecule to water at different proton concentra-

tions. The full curves in the upper panel show raw time-correlated single-photon counting data, corrected for the finite radiative lifetime of the excited dye molecule, after subtraction of the equilibrium plateau as determined numerically from it.[15] At each of the four proton concentrations, a sixth order polynomial has been fitted to the data on the log–log scale for smoothing purposes (dashed curves).

The logarithmic derivatives, Eq. (20), determined by analytic differentiation of the polynomial fits are shown in the bottom panel of Fig. 3. The appearance of a maximum in $B(t)$ at intermediate times for high proton concentrations is in striking similarity to the Brownian dynamics results. The difference in spatial dimensionality ($d=1$ for the simulations as opposed to $d=3$ for experiment) or in interparticle interactions (neutral vs charged particles) could lead to quantitative differences but the qualitative effect should hold irrespectively. The measured long time behavior remains unclear due to statistical noise. On the basis of our simulations, one may predict that $B(t)$ should tend to 3/2 (or to a value very close to 3/2) at infinitely long times. It would be interesting if the maximal count number could be increased tenfold to check this prediction experimentally.

We conclude by reiterating the somewhat unexpected observation encountered in this work: The most prominent effect of many-body dynamics on a reversible reaction seems to be neither at infinitely short nor at infinitely long times but at intermediate times, where a steep power-law phase emerges with increasing particle concentration. This intermediate phase is described only qualitatively by approximate theories and requires full Brownian dynamics (or more elaborate theories) for its elucidation. With increasing cK_{eq}, this phase may resemble an exponential decay to equilibrium in three-dimensional systems. Although there would be an ultimate switch over to the power-law behavior, this asymptotic limit will become increasingly more difficult to observe. This could explain why for slow reactions conventional chemical kinetics is successful in describing the time course of the reaction.

Reversible binding is an important elementary step in fundamental processes in fields as diverse as analytical and biophysical chemistry. It serves in chromatographic columns for differential separation of solutes according to their (reversible) adsorption isotherms; it is the primary step of substrate binding to an enzyme; it is pivotal in hormone and neuro-transmitter binding to their receptors. Thus the double-power-law phenomenon may be of interest when quantitative analyses of such systems are undertaken.

ACKNOWLEDGMENTS

We thank Attila Szabo for helpful correspondence. Work supported by grants from the Israel Ministry of Absorption (A.L.E.) and the Zevi Hermann Schapira Research Fund. The Fritz Haber Research Center is supported by the Minerva Gesellschaft für die Forschung, München, Germany.

[1] S. Lee and M. Karplus, J. Chem. Phys. **86**, 1883 (1987).
[2] N. Agmon and A. Szabo, J. Chem. Phys. **92**, 5270 (1990).
[3] J. Vogelsang and M. Hauser, Ber. Bunsenges. Phys. Chem. **94**, 1326 (1990).
[4] S. F. Burlatsky, G. S. Oshanin, and A. A. Ovchinnikov, Chem. Phys. **152**, 13 (1991).
[5] A. Szabo and R. Zwanzig, J. Stat. Phys. **65**, 1057 (1991).
[6] A. Szabo, J. Chem. Phys. **95**, 2481 (1991).
[7] N. Agmon, H. Schnörer, and A. Blumen, J. Phys. Chem. **95**, 7326 (1991).
[8] A. Molski and J. Keizer, J. Chem. Phys. **96**, 1391 (1992).
[9] W. Naumann, J. Chem. Phys. **98**, 2353 (1993).
[10] N. Agmon, Phys. Rev. E **47**, 2415 (1993).
[11] T. R. Waite, Phys. Rev. **107**, 463 (1957).
[12] L. Monchick, J. L. Magee, and A. H. Samuel, J. Chem. Phys. **26**, 935 (1957).
[13] J. Yguerabide, J. Chem. Phys. **47**, 3049 (1967).
[14] N. Agmon, E. Pines, and D. Huppert, J. Chem. Phys. **88**, 5631 (1988).
[15] D. Huppert, S. Y. Goldberg, A. Masad, and N. Agmon, Phys. Rev. Lett. **68**, 3932 (1992).
[16] A. Szabo, R. Zwanzig, and N. Agmon, Phys. Rev. Lett. **61**, 2496 (1988).
[17] A. L. Edelstein and N. Agmon, J. Chem. Phys. **99**, 5396 (1993).
[18] N. Agmon, J. Chem. Phys. **81**, 2811 (1984).
[19] E. Pines, D. Huppert, and N. Agmon, J. Chem. Phys. **88**, 5620 (1988).